CREEP CRACK GROWTH BEHAVIOR OF P91 STEEL WELDMENTS

by

Mohamed SWEI[a*], Aleksandar S. SEDMAK[a], Blagoj PETROVSKI[a], Zorana Z. GOLUBOVIĆ[b], Simon A. SEDMAK[b], Marko KATINIĆ[c], and Khaled I. AZZABI[d]

[a] Faculty of Mechanical Engineering, University of Belgrade, Belgrade, Serbia
[b] Innovation Center of the Faculty of Mechanical Engineering, Belgrade, Serbia
[c] Faculty of Mechanical Engineering, Josip Juraj Strossmayer University of Osijek, Slavonski Brod, Croatia
[d] Janzour College of Engineering Technology, Tripoli, Lybia

Original scientific paper
https://doi.org/10.2298/TSCI170729240S

The steels operating at elevated temperatures are well known to be exposed to premature failure due to cracking caused by constant thermal stress, i. e. secondary creep process. Therefore, creep crack growth tests were carried out on compact tension specimens machined from P91 weld joint at 600 °C to determine its behavior in realistic conditions. At the same time, numerical method for predicting the creep crack growth in compact tension specimens by a series of incremental steady-state finite element analysis were performed using Norton's law to represent creep behavior. Verification of the finite element predictions were obtained for weld metal and heat affected zone by comparison with experimental results, indicating at the same time that creep crack growth rates are significantly higher for weld metal than for base metal.

Key words: *creep crack growth, thermal stresses, P91 steel weldment*

Introduction

Steel weldment components used in power generation plants are continually exposed to high temperatures and failure processes such as creep crack growth (CCG), which can occur within the high temperature regime. Safe and accurate methods to predict CCG are therefore required in order to assess the reliability of such components, [1]. Finite element (FE) methods has been applied extensively in the study of CCG to predict the fracture mechanics parameters in estimating CCG rates, [2-6], as well as some analytical and empirical methods to predict creep strain, [7-11].

This approach is of utmost interest for critical components in thermal power plants, such as steam-lines. Creep damage and crack growth is typical problem for steam-lines operating at high temperatures (550 °C and higher), being heavily loaded at the same time. Remaining life of critical components, including steam-line, is very important topic for many old thermal power plant, which are already operating over their design life time. Having in mind that operating parameters, like temperature and stress, directly affect the life of a steam-line, it is clear that one has to pay attention to these effects, focused on different weldment region,

* Corresponding author, e-mail: mohmswei@hotmail.com

since they are typically location where damage and crack would appear first. Therefore, our main topic here is CCG rate in different weldment regions, correlated with the fracture parameter, C^*, to evaluate behavior of a critical component's regions and their residual life, as shown also in [3, 8].

It is well known that CCG rates, da/dt, correlate very well with the creep fracture parameter, C^*, for homogeneous material, [2]. Experimental studies on the CCG in weldments have shown that the C^* parameter can also be used for characterizing the CCG in weldments. Tests have been carried out, following the ASTM E1457-00 standard [12], using compact tension (CT) specimens for P91 weldments. The experimental data obtained were used to investigate the CCG behavior of welds and to validate numerical methods used for crack growth modelling.

In this paper, CCG tests were carried out on CT specimens machined from P91 weld joints at 600 °C. This steel is referred to as model 9Cr1Mo or P91 and is used for manufacturing pipes and vessels for a fast breeder reactor. This steel has found wide application in all new Japanese and European power stations for the manufacture of pipes and small forgings, [13]. It is tough, readily weldable and it has high creep strength at 600 °C and 100000 hours.

The creep damage approach can be used with finite element (FE) analysis to predict the CCG behavior of welds [14]. However, this method demands large number of material constants, which are difficult to provide especially for the heat-affected zone (HAZ) material. Rather, a relatively simple numerical method for CCG prediction has been investigated and validated using experimental results. Namely, Norton's law, which requires only two material constants, has been used to predict the CCG in CT specimens made of P91 weldments and compared with experimental data for verification.

Experimental analysis

Standard creep test specimens were machined from the welded joint and from simulated HAZ materials of P91 steel. Crack growth test specimens were machined from the base metal and weldments with the notches introduced centrally, using electrical discharge method (EDM) in WM and HAZ, as shown in [14].

Test data for different temperatures

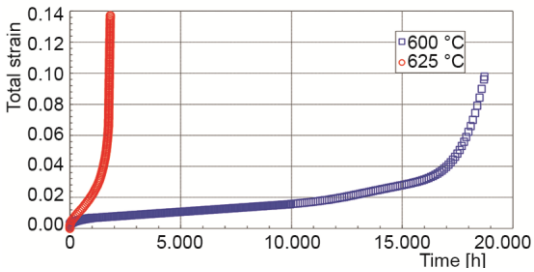

Figure 1. Strain *vs.* time for different temperatures

The P91 steel has been also tested at somewhat higher temperatures to find the upper limit of its applicability. Results for strain *vs.* time, at two different temperatures, 600 °C and 625 °C, are given in fig. 1. They clearly indicate detrimental effect of temperature, limiting P91 usage to 600 °C.

Test data for weldment zones

To obtain the material properties for the base metal (BM), WM, and HAZ regions, tensile specimens of were machined out of the butt-welded pipe segments by EDM technique, and presented in tab. 1, together with data for Norton's law material constants. It can be seen in tab. 1 that the variation in creep properties does not follow the same sequence as the yield strength data. The creep exponent, n, is the lowest for the WM whereas the HAZ has the lowest m value determined in tensile tests.

Table 1. Material data determined in tensile and creep tests

Material	$R_{0.2}$ [MPa]	R_m [MPa]	E [GPa]	D_1	m	A_1	n
P91 BM-600°C	441	464	164	0.0018	27.73	$1.57 \cdot 10^{-45}$	18.51
P91 WM-600°C	362	385	125	0.0015	23.86	$5.99 \cdot 10^{-24}$	8.55
P91 SIM. HAZ-600°C Type IV	320	333	155	0.0016	17.38	$7.16 \cdot 10^{-35}$	14.35
P91 SIM. HAZ-600°C Centre	293	317	139	0.0016	17.38	$7.16 \cdot 10^{-35}$	14.09

Creep crack growth test

The CCG tests were performed according to the ASTM standard E1457-08, [12]. The crack length and load line displacement were measured, an DC electrical current was applied to the specimen and the value of the electric potential drop was measured, determination of Δa, by using PD method compliance. The specimen used were CT25 type with W = 25 mm, with grooves of 20% of specimen thickness, to provide a crack straight front. The CT specimen prepared for testing connected through sensors for potential current measurement of displacement and potential drop as indicated in fig. 2. The results are shown in fig. 3 for BM, WM and HAZ of P91 steel.

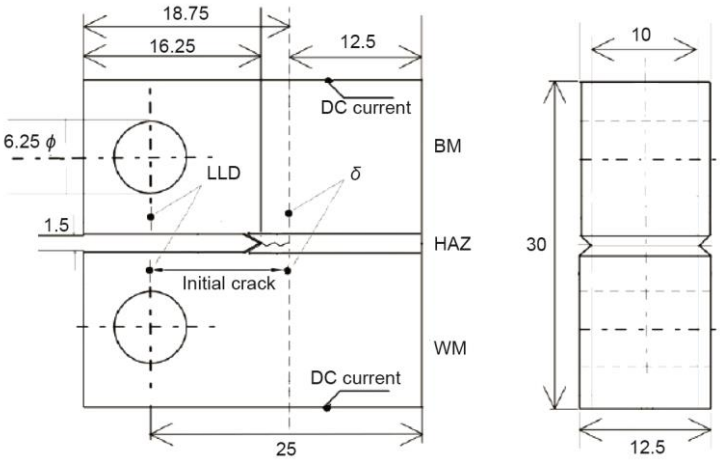

Figure 2. Dimensions and arrangement of tested CT specimen

This data was used in calculating C^* and for validating the FE damage predictions. Comparing the CCG for both steels it can be seen that larger Δa can be obtained in creep weak weldment regions relative to base metal and the gradual increase in the crack length with time while it is faster in weld metal and heat affected zone.

Weldments test data and creep behavior

The creep and creep rupture curves for the P91 weldments are shown in figs. 4 and 5, for different levels of stress.

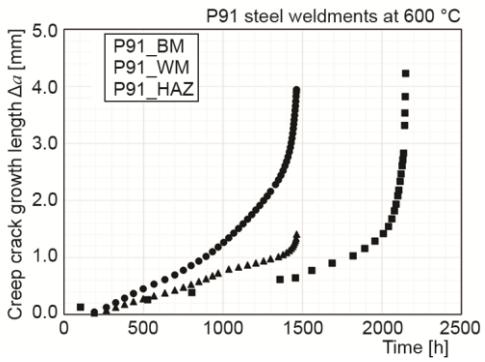

Figure 3. The CCG comparison of P91 weldments

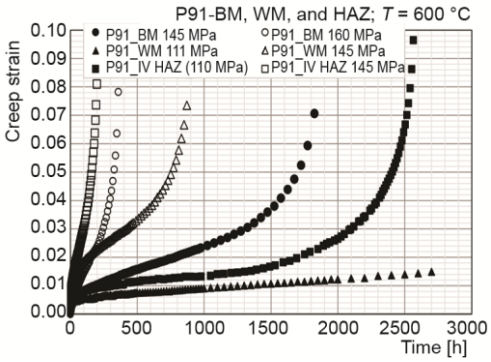

Figure 4. Creep behavior of P91 weldments at T = 600 °C

*Determination of C**

The experimental C^* parameter for the CT specimen is estimated from the creep load line displacement rate, $\dot{V}_c$, using the equation:

$$C^*(t) = \frac{n}{n+1}\frac{P\dot{V}_c}{B_n(W-a)}\left[2+0.522\left(1-\frac{a}{W}\right)\right] \tag{1}$$

where P is the applied load, W – the specimen thickness, a – the crack length, and B_n – the net thickness of the side grooved specimen. Also n is the creep stress exponent in the Norton creep law given by:

$$\dot{\varepsilon}_{\min} = A\sigma^n \tag{2}$$

The n exponent values are given in tab. 1 for each weldment zones, having higher values for base metal, but the materials exhibit creep deformations at elevated temperature would be better presented by average creep strain rates covering all three regimes of creep as described schematically in fig. 6.

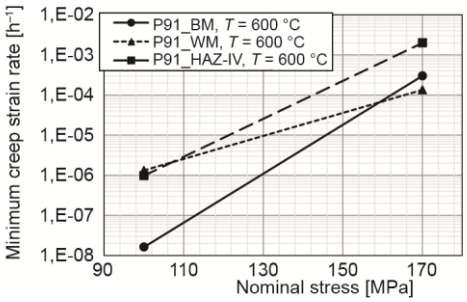

Figure 5. Minimum creep strain rate data of P91 weldments at T = 600 °C

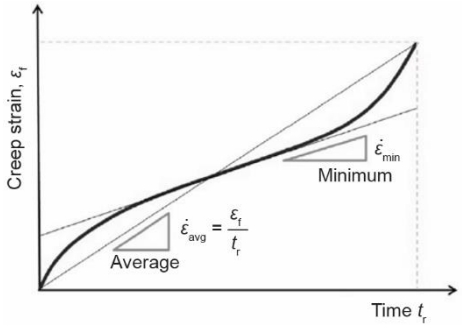

Figure 6. Creep curve representing secondary creep rate and average creep rate

The average creep rate is relatively more suitable method to yield more representative deformations rates for longer times defined by:

$$\dot{\varepsilon}_{\text{avg}} = \frac{\varepsilon_f}{t_r} = \dot{\varepsilon}_0 \left(\frac{\sigma}{\sigma_0} \right) = A_{\text{avg}} \sigma^{n_{\text{avg}}} \tag{3}$$

The experimental data for CT specimens show the C^* parameter correlates the crack growth rate data, a, and the behavior can be written in a simplified form:

$$\dot{a} = DC\phi \tag{4}$$

where D and ϕ are material constants, which are presented numerically in equations in tab. 2, and are fitted by C^* in fig. 7.

The CCG rates of different weldment zones of P91 at 600 °C are correlated crack tip parameter, C^*, show consistency in correlations after the steady-state CCG conditions at the crack tip have been established. Comparison of CCG rates correlations of different weldment zones of P91 steel at 600 °C, directs attention to lower resistances of P91 weldment zones than that of P91 base metal. Also, fig. 7 indicates bigger scatter of HAZ results compared to the BM and significantly higher crack growth rates that are represented by best fit for weldments data, tab. 2.

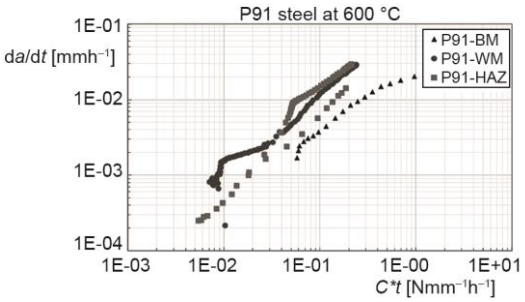

Figure 7. Relationship between C^* and CCG rate of P91 weldments

Table 2. Weldments data

	P91	WM/BM	HAZ/BM	Eq.
BM	$\dot{a} = 0.0284(C^*)^{0.871}$	≈ 4	≈ 6	(5)
WM	$\dot{a} = 0.1143(C^*)^{1.0087}$			(6)
HAZ	$\dot{a} = 0.2547(C^*)^{1.3124}$			(7)

For the same values of C^*, the CCG rates for weld metal and heat affected zone are higher than for base metal by a factor of ≈4 and ≈6, respectively.

Finite element modelling of creep crack growth

The method implemented in this study is the nodal release in the crack path assuming a straight-line crack path for incremental increase.

Modified nodal release method

The advantage of this method that only the material constants in Norton's law is required to determine the CCG and C^* parameter, a sequence of incremental steady-state FE analysis, with increasing crack lengths to simulate continuous crack propagation. The starting constraint was applied to the W = 25 mm and W = 50 mm CT specimens models with initial crack length of 12.5 mm and 25 mm, respectively. As seen in fig. 8, applied in the y-direction (crack path) equally to experimental value for first step in FE model, the incremental increase in crack length is set for 0.5 mm to represent the increase in Δa.

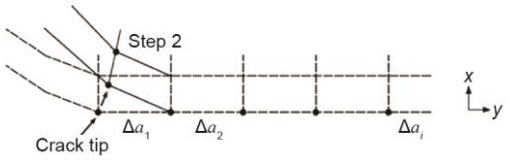

Figure 8. Schematic of node release modeling for creep crack growth

Finite element models

The CCG simulations were carried out using the FE program ABAQUS, 2-D FE analyses were performed to calculate the C^* for base metal, weld metal and heat affected zone.

Due to the symmetry of CT models, only one-half of BM, WM, and HAZ were considered, as shown in fig. 9, the FE mesh mainly consists of 2-D, (CPS8R) an 8-node biquadratic plane stress quadrilateral, reduced integration, the element size nearst to the crack front of 0,123 mm, to provide adequately accurate results.

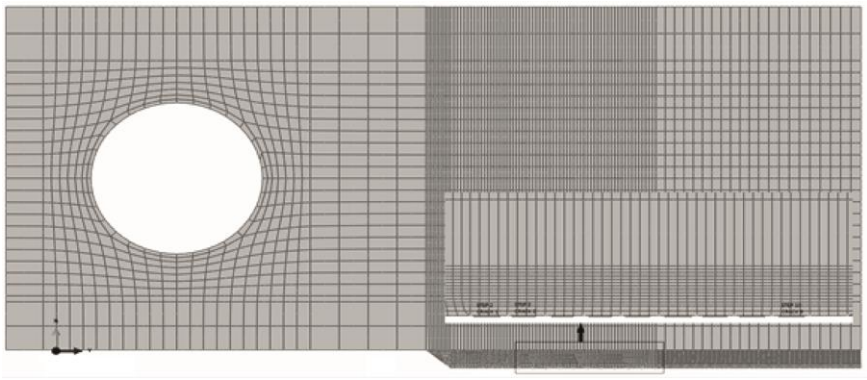

Figure 9. The 2-D FE modeling of CT specimen for CCG

The procedure followed was to divide the crack front into nine cracks over 9 steps. For total Δa = 4.5 mm by increment of 0.5 mm for each crack at mesh size of 0.1 mm, calculated C_t integral for each step starting at Step 2.

The results obtained by using described procedure are shown in figs. 10 and 11, together with the experimental results. One can see relatively large difference, especially in the case of plain strain 2-D simulation. Anyhow, relatively good agreement between experimental results and 2-D plain stress simulation is encouraging for further investigations.

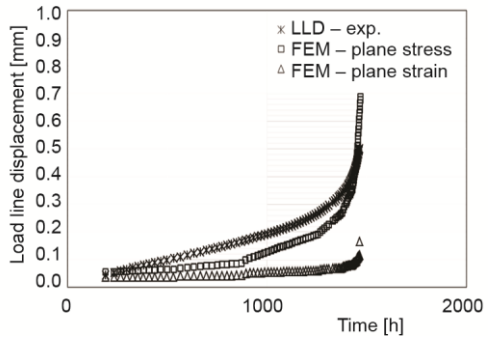

Figure 10. Load-line displacement *vs.* time obtained from experimental and FE analysis

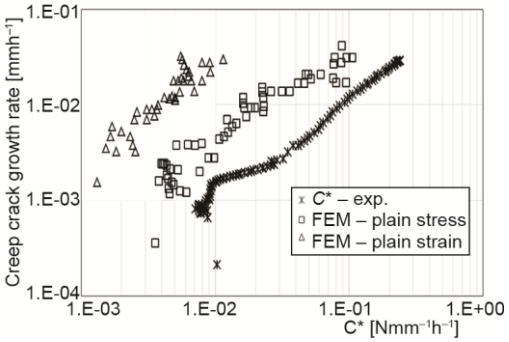

Figure 11. Comparison of FEM calculated CCG rate *vs.* experimental data

Conclusions

On the basis of the results shown one can conclude as following.

- Temperature effect on creep strain rate is very strong, limiting P91 usability to 600 °C. Namely, at 625 °C strain rate is approximately 10 times higher than at 600 °C.
- Creep crack growth rate can be correlated with C^* fracture parameter, indicating lower crack growth resistance of weldment regions as compared to the base metal.
- Having in mind the simplicity of the finite element modeling used here, the agreement between experimental results and 2-D plain stress simulation is good enough. Nevertheless, more investigation is needed, including a 3-D simulation to achieve better agreement with experimental results.

References

[1] Dogan, B., *et al*., Significance of Creep Crack Initiation for Defect Assessment, *Proceedings*, Int. FESI Conference ESIA7-Integrity for Life, Manchester, UK, 2004, pp. 335-346
[2] Yatomi, M., Tabuchi, M., Issues Relating to Numerical Modelling of Creep Crack growth, *Engineering Fracture Mechanics, 77* (2010), 15, pp. 3043-3052
[3] Sedmak, A., *et al*., Finite Element Modelling of Creep Process – Steady-State Stresses and Strains, *Thermal Science, 18* (2014), Suppl. 1, pp. S179-S188
[4] Hyde, T. H., *et al*., A Simpliified Method for Predicting the Creep Crack Growth in P91 Welds at 650 °C, *Proceedings, Ins. of Mech. Eng., Part L, Journal Materials Design and Applications, 1* (2010), 4, pp. 1-12
[5] Katinić, M.; *et al*., Numerical Analysis of the Effect of Initial Plasticity on Transient Creep in Compact Tension Specimen under Mechanical Load, *Technical Gazette, 23* (2016), 5, pp. 1417-1421
[6] Katinić, M., *et al*., A Numerical Creep Analysis on the Interaction of Twin Parallel Edge Cracks in Finite width Plate under Tension, *Thermal Science, 18* (2014), Suppl. 1, pp. S159-S168
[7] Damnjanović, A., *et al.*, Integral Evaluation by Using EPRI Procedure, *Structural Integrity and Life, 1-2* (2002), Jan., pp. 51-54
[8] Gupta, N., *et al.*, Mathematical Method to Determine Thermal Strain Rates and Displacement in a Thick-Walled Spherical Shell Structural Integrity and Life, *Structural Integrity and Life, 16* (2016), 2, pp. 99-104
[9] Gupta, N., *et al.*, Creep Modelling in a Composite Rotating Disc with Thickness Variation in the Presence of Residual StressStructural Integrity and Life, *Structural Integrity and Life, 16* (2016), 2, pp. 105-112
[10] Pankaj, T., Analysis of Thermal Creep Stresses in Transversely Thick-Walled Cylinder Subjected to Pressure, *Structural Integrity and Life, 15* (2015), 1, pp. 19-26
[11] Pankaj, T., *et al.*, Thermo Elastic-Plastic Deformation in a Solid Disk with Heat Generation Subjected to Pressure, *Structural Integrity and Life, 15* (2015), 3, pp. 135-142
[12] ***, ASTM E1457-00, Standard test method for measurement of creep crack growth rates in metals, ASTM 03.01, Philadelphia: ASTM 2000, Penn., USA, 19103
[13] Abe, F., *et al*., *Creep-resistant steels*, CRC Press, Boca Raton, Fla., USA, 2008
[14] Dogan, B., Petrovski, B., Creep Crack Growth of High Temperature Weldments, *International Journal of Pressure Vessels and Piping, 78* (2001), 11-12, pp. 795-805

Paper submitted: July 29, 2017
Paper revised: November 15, 2017
Paper accepted: November 17, 2017